

Valorization of glycerol into triacetin: Green innovation in sustainable biodiesel additive development for ecological stability

Nuryoto Nuryoto^{1*}, Soni Candra¹, Widya Ernayati Kosimaningrum¹,
Rafif Nur Tahta Bagaskara²

¹ Chemical Engineering Department, Faculty of Engineering, Universitas Sultan Ageng Tirtayasa, Jl. Jendral Sudirman KM. 3, Cilegon, Banten 42435, Indonesia

² School of Environment, Faculty of Arts and Science, University of Toronto, 33 Willcocks Street, Suite 1016V, Toronto, ON, M5S 3E8, Canada

* Corresponding author's e-mail: nuryoto@untirta.ac.id

ABSTRACT

To ensure stable high prices for glycerol, it is essential to process glycerol into high-value products. The low price of glycerol and the high cost of its separation could potentially turn glycerol into waste, ultimately disrupting ecological stability. However, converting glycerol into triacetin through a reaction with acetic acid poses challenges due to the presence of water in the reaction system. Water is a byproduct of triacetin synthesis. The presence of water can significantly reduce reaction performance, causing reverse reactions toward reactants and hindering the diffusion-reaction process, which is the core stage in triacetin synthesis. Therefore, this research was conducted to analyze the phenomenon and the extent of water's influence on the performance of triacetin synthesis reaction based on the acetic acid conversion produced. Additionally, this research attempts to model the reaction process with a simple mathematical model to understand the phenomena occurring. Observations were conducted using two different batch reactors: one equipped with a condenser (which allowed for water condensation) and the other without a condenser (where water evaporated). The reactions were carried out at temperatures ranging from 90 to 110 °C for 4 hours, with a stirring speed of 700 rpm. The reactant ratio varied between 1:3 and 1:5 mol of glycerol per mole of acetic acid. Reaction results were analyzed using acid-base titration and GC MS for acetic acid conversion and the percentage of triacetin produced. This research demonstrated that increasing the reactant ratio to 1:3 mol of glycerol per mole of acetic acid at 90 °C and raising the reaction temperature positively influenced the conversion of acetic acid. The reactor without a condenser achieved significantly higher acetic acid conversion compared to the reactor with a condenser, and the optimal reaction kinetics model identified was the second-order kinetics model. This research provides good information regarding the influence of water on reaction performance in triacetin synthesis. The aim of this research is to collaborate with prior studies to enhance the understanding of the triacetin synthesis process. Further observation is needed, as the main product, triacetin, produced is still relatively small compared to the intermediate products, monoacetin and diacetin.

Keywords: esterification, reaction, natural zeolite, pretreatment, heterogeneous.

INTRODUCTION

Biodiesel as an energy blend has been proven to reduce gas emissions compared to fossil fuels without biodiesel mixture (Khalaf et al., 2024). Environmental issues and global warming have led many countries such as America, Brazil, the European Union, and Indonesia (Eremeeva et al., 2023; Wirawan et al., 2024) to start implementing energy blends between fossil fuels and biodiesel.

This condition affects the increase in global biodiesel production. In 2021 alone, global biodiesel production reached 40 million tons (Eremeeva et al., 2023) and experienced an increase of about 50% to 60.7 million tons in 2022 (Awogbemi and Kallon, 2023). The biodiesel production process always produces a by-product in the form of glycerol, amounting to 10% of the biodiesel production capacity (Pandit et al., 2023). So, it can be interpreted that for every 100 liters of biodiesel

produced, about 10 liters of glycerol will be generated. As biodiesel production continues to increase due to rising biodiesel consumption, the amount of glycerol produced will automatically increase as well. According to economic law, if a product is abundant in the market but the demand of that product remains constant, the potential price of that product will decrease. However, the process of purifying glycerol to achieve marketable glycerol requires significant costs. This is because the glycerol purification process requires a long route through the separation process in the distillation unit. The feared condition is that glycerol will be considered no longer economical and will become waste, potentially being discarded into the environment. This event is certainly not desired by either biodiesel producers or the community, because if this happens, it will cause environmental pollution.

Based on studies conducted by Rahmat et al., 2010 and Sriratchachawan et al. (2022) during the period of 2003–2020, it was shown that the increase in glycerol production has significantly impacted the decrease in selling price of glycerol products

in the market. The selling price of glycerol, which was initially around 36 cents/liter in 2003, dropped to 9 cents/liter in 2020 (Sriratchachawan et al., 2022). This condition is very concerning if preventive action is not taken immediately, namely by preparing alternative technologies for processing glycerol into other more economical products. Diversification of glycerol processing into other products will increase the absorption of glycerol itself, so that the price of glycerol remains stable, and the concept of *zero waste* in biodiesel production can be achieved. In this research, an attempt is made to process glycerol into a biodiesel additive in the form of triacetin compound. The synthesis of triacetin itself basically follows the concept of esterification reaction, where the reaction occurs between glycerol and acetic acid to form triacetin as presented in Figure 1.

The details of Figure 1 can be described as shown in Figure 2, where triacetin can be formed through a 3-step reaction. In the first step, glycerol (G) and acetic acid (AA) react to form monoacetin (MA) + water, in the second step, MA and

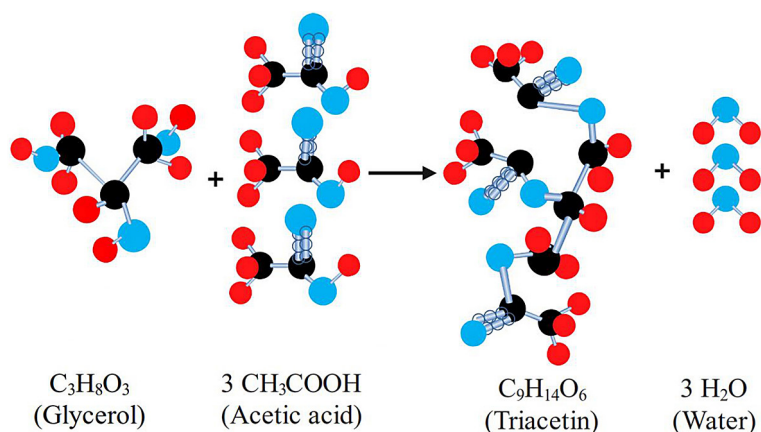


Figure 1. Illustration of the reaction between glycerol and acetic acid to form triacetin and water

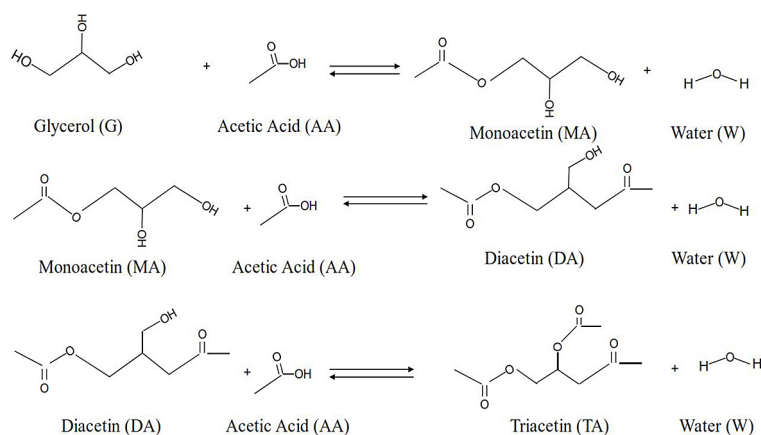


Figure 2. Illustration of triacetin synthesis

AA react to form diacetin (DA) + water, and finally, DA reacts again with AA to form triacetin (TA) + water (W) (Sandid et al., 2024).

The diversification of glycerol into triacetin, based on economic studies, turns out to be very profitable. According to a simulation by Pandit et al. (2023), the production of triacetin from glycerol can generate a gross profit margin (GPM) of \$60.5 million/year (based on calculations for 100,000 tons of glycerol). Moreover, based on technical studies, when triacetin is added to fossil fuel + biodiesel (biodiesel blend), it produces significantly lower gas emissions compared to

biodiesel without triacetin (Kalyani et al., 2023). Observations conducted on B20 biodiesel (80% fossil fuel and 20% biodiesel) + 2% triacetin showed a reduction in NOx by 27.5% and CO by 45.95% compared to emissions from B-20 combustion (Çakmak, 2021). Therefore, based on economic assessments and technical tests, triacetin is worthy of further development.

Essentially, research related to triacetin from glycerol has been conducted (Table 1). Based on the literature review, no studies have been found examining the impact of water compounds in the reaction system on the performance of triacetin

Table 1. Synthesis of triacetin using glycerol and acetic acid

Raw materials	Operational condition	Research results	References
Glycerol and acetic acid with aluminum and silica catalysts extracted from clay using NaOH and HCl	Reactant ratio of 1:6.6 to 1:11.5 mol of glycerol per mole of acetic acid, reaction temperature of 90 °C, catalyst concentration of wt%, stirring speed set at 300 rpm, reaction time of 3 hours, using a batch reactor with a catalyst size of 90 mesh	The optimum condition was achieved at 1:1.89 mol of glycerol per mole of acetic acid with a glycerol conversion of 87.40% using a silica catalyst	Yanti et al., 2019
Glycerol and acetic acid with CeO ₂ -ZrO ₂ based catalyst	Reactant ratio of 1:3 to 1:20 mol of glycerol per mole of acetic acid, reaction temperature of 70 to 110 °C, catalyst concentration of 1 to 7 wt%, constant stirring speed, reaction time of 5 hours, using a circulating batch reactor	The optimum condition was achieved at 1:10 mol of glycerol per mole of acetic acid, 5wt% catalyst, and reaction temperature of 100 °C with glycerol conversion of 99.12% and triacetin selectivity of 21.26%	Kulkarni et al., 2020
Glycerol and acetic acid with silica-based catalyst from rice husk	Reactant ratio of 1:3 mol of glycerol per mole of acetic acid, reaction temperature of 100 °C, catalyst concentration of 5 wt%, stirring speed set at 400 rpm, reaction time of 0.5 hours, using a batch reactor with microwave assistance	The monoacetin, diacetin, and triacetin produced are 39.9%, 56.9%, and 3.1% respectively	Tasuna and Hidayatillah, 2021
Glycerol and acetic acid with Pd/AC-based catalyst	Reactant ratio of 1:5 to 1:10 mol of glycerol per mole of acetic acid, reaction temperature of 80 to 110 °C, catalyst concentration of 0.5 to 2.5 wt%, stirring speed set at 400 rpm; reaction time of 1.5 hours, using a batch reactor in a microwave	The optimum condition was achieved at 1:10 mol of glycerol per mole of acetic acid, 0.718t% catalyst, and reaction temperature of 110 °C with glycerol conversion of 96.64% and triacetin selectivity of 0.231%	Azmi et al., 2023
Glycerol and acetic acid with Amberlyst 36 catalyst	Reactant ratio of 1:6 to 1:12 mol of glycerol per mole of acetic acid, reaction temperature of 100 to 130 °C, catalyst concentration of 2.5 to 7.5 wt%, stirring speed set at 100 to 800 rpm, reaction time of 8 hours, using a batch reactor	The optimum condition was achieved at 1:9 mol of glycerol per mole of acetic acid, catalyst 5wt%, and reaction temperature of 120 °C with glycerol conversion of approximately 98% and triacetin selectivity of approximately 27%	Sandid et al., 2024.
Glycerol and acetic acid with Cs _{2.5} H _{0.5} PW ₁₂ O ₄₀ /K-10 (Cs-DTP-K10) catalyst	Reactant ratio of 1:9 mol of glycerol per mole of acetic acid, reaction temperature of 120 °C, stirring speed set at 800 rpm, reaction time of 4 hours, catalyst concentration of 0.01 g/cm ³	A glycerol conversion rate of 92% was achieved, resulting in the production of acetin, diacetin, and triacetin	Yadav and Katole, 2025
Glycerol and acetic acid with biochar acid catalyst	Reactant ratio of 1:6 mol of glycerol per mole of acetic acid, reaction temperature of 100 °C, reaction time is 4 hours, catalyst amount of 150 mg	90% glycerol conversion resulted in the formation of acetin, diacetin, and triacetin, comprising 42.2%, 53.4%, and 4.2% respectively	Jagadish et al., 2025

synthesis. This research aims to observe the actual phenomena that occur due to the presence of water in the reaction system during the triacetin synthesis process. Specifically, it focuses on how water affects the conversion of reactants, mainly the acetic acid produced. For this purpose, observations were conducted with a batch reaction system using two different equipment setups. First, the reaction was carried out by installing a condenser on the reaction system so that evaporated water returns to the reaction system. Second, the reaction was carried out without a condenser, allowing the water to evaporate into the environment. Theoretically, water is a byproduct of this reaction (Fig. 1), and the presence of water will disrupt the diffusion-reaction process between reactants and catalysts. This occurs because glycerol and acetic acid dissolve well in water, creating a barrier that prevents the reactants from diffusing and reacting. This condition will affect the reaction rate and performance of the reaction. Additionally, when reactants dissolve in water, especially reactants in the form of acetate, it will interfere with the interaction between acetic acid and intermediate products such as monoacetin or diacetin to form triacetin (referring to the reaction stages in Fig. 2). Therefore, this research was conducted to analyze the phenomena and the extent of water's influence on the performance of the triacetin synthesis reaction based on the conversion of the produced acetic acid. Furthermore, this research also aims to develop a simple mathematical model to understand better the reaction process and the phenomena occurring. The results of this research will provide additional information and complement previous studies on triacetin synthesis to develop further triacetin synthesis toward a more effective, efficient, and economical reaction process. The activated clinoptilolite type natural

zeolite from Lampung, Indonesia, is utilized as a catalyst in this research to use of abundant local resources that have not been maximally benefited from. This research focuses on the effects of reaction temperature and the ratio of reactants. This matter is based on the concept that the reaction rate in liquid-solid reactions will be influenced by temperature and reactant ratio factors. In simple terms, the diffusion-reaction process in this study can be illustrated in Figure 3. Referring to Figure 3 (Fogler, 2006), if the system has reached steady-state conditions, the external diffusion rate is equal to the internal diffusion rate, which is also equal to reaction rate. Under these conditions, the reaction rate can be expressed with Equation 1 and Equation 2.

$$\frac{dC}{dt} = D \frac{dC}{\delta} = D_e \frac{dC}{dr} = k C_r^n \quad (1)$$

$$\frac{dC}{dt} = k_c (C - C_b) = k_e (C - C_r) = k C_r^n \quad (2)$$

where: $D \frac{(C-C_b)}{\delta}$ – external diffusion (mol/dm³ s), $k C_r^n$ – esterification reaction rate (mol/dm³ s), $D_e \frac{(C-C_r)}{dr}$ – internal diffusion (mol/dm³ s), D and D_e – external esterification reaction rate (dm²/s), C_b and C_r – reactant concentrations in outer layer of catalyst and inside the catalyst bulk (mol/dm³), δ – film layer (dm), r – catalyst radius (dm), k – reaction rate constant (1/s (mol/dm³)ⁿ⁻¹), n – reaction order (dimensionless), k_c and k_e – external mass transfer constant and internal mass transfer constant (1/s).

The temperature parameter (T) will affect the value of the diffusivity coefficient (D) according to the Wilke-Chang formula (Putera et al., 2024), and the reaction rate constant (k) refers to the Arrhenius equation (Amr et al., 2023; Okonye et al., 2023). Thus, by integrating the temperature

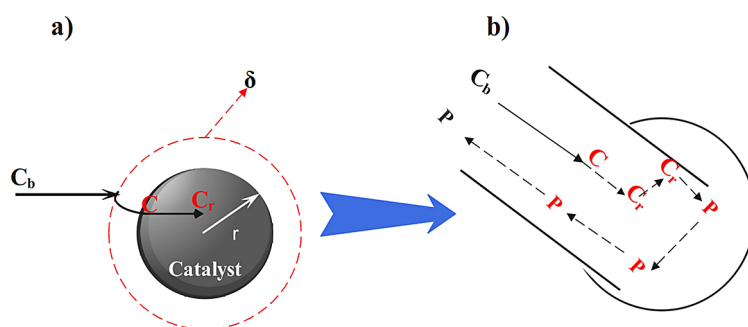


Figure 3. Illustration of: (a) diffusion-reaction in the esterification reaction between glycerol and acetic acid with natural zeolite catalyst, and (b) step by step process of reactants (glycerol and acetic acid – C) diffusing and reacting to form products (Triacetin and water – P)

parameter and reactant concentration, it is expected that the reaction rate and the resulting triacetin product will be maximized, resulting in effective and efficient operating conditions.

The selection of natural zeolite in the form of clinoptilolite natural zeolite from Lampung, Indonesia (Intang et al., 2024; Al Muttaqii et al., 2024) as a catalyst in this research is because this zeolite has a fairly good performance as a catalyst (Al Muttaqii et al., 2024; Hasanudin et al., 2024), although pretreatment is indeed necessary before use so that the diffusion-reaction process can proceed quickly.

MATERIALS AND METHODS

Materials and research equipment

The raw materials used included acetic acid of the Merck brand with 96% concentration, purchased from the Shopee-Indonesia marketplace. The Glycerol used was technical grade glycerol with 99% concentration, also purchased from the Shopee-Indonesia marketplace. Natural clinoptilolite zeolite, used as a catalyst, was obtained from Lampung-Indonesia. Before use, the zeolite underwent pretreatment with 6 N sulfuric acid. This pretreatment was performed to remove impurities contained within and to increase the acidity and surface area of the zeolite. The expectation was that the diffusion-reaction process in triacetin synthesis could proceed quickly, and the resulting triacetin product would be maximized. The reaction process in this study was conducted using a batch reactor, which consists of: (1) Three-neck

flask, (2) heating mantle, (3) condenser, (3') hose, (4) overhead stirrer motor, (5) thermometer, (6) sample collector, (7) sample container, (8) stirrer, (9) beaker. The schematic of the equipment used in this study is illustrated in detail in Figure 4.

Zeolite preparation

Natural clinoptilolite zeolite from Lampung-Indonesia with a size of - 45 + 60 mesh (referring to Ramadhan et al., 2019, and Nindya et al., 2020) was activated using sulfuric acid solution with a concentration of 6 N (made from 98% Merck sulfuric acid by dissolving it in a certain volume of distilled water) with a ration between zeolite mass and sulfuric acid solution of 10 grams/100 ml of sulfuric acid solution. The activation process was carried out for 2 hours at an activation temperature of 110 °C, while stirring at 600 rpm. The activated natural zeolite was filtered using filter paper, then washed using distilled water until the pH of the distilled water before use (approximately 4 rinses). In the next stage, the natural zeolite was drained and placed in an oven at 200 °C for 2 hours. After that, the natural zeolite was removed from the oven and the zeolite was ready to be used as a catalyst. To observe the impact of the activation process that had been carried out on the zeolite, characterization was performed on both the natural zeolite before and after activation. Zeolite characterization was done using scanning electron microscope (SEM), Fourier-transform infrared spectroscopy (FTIR), surface area analyzer (SAA), and TPD-NH₃ tests.

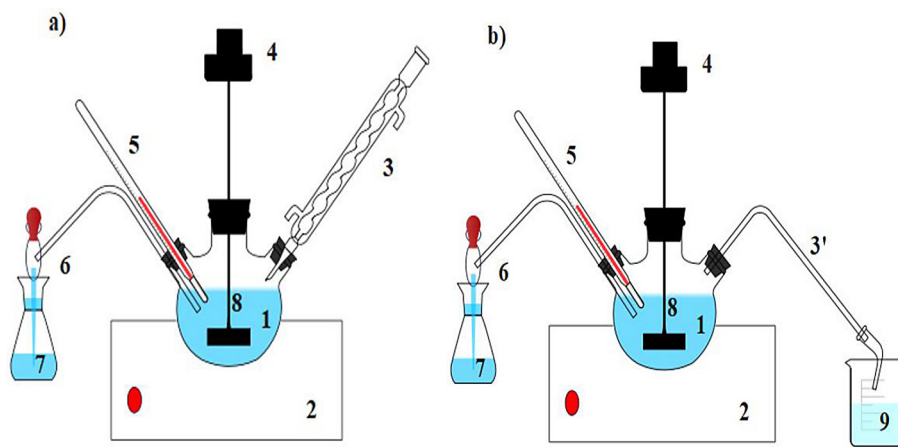


Figure 4. Schematic illustration of research equipment: (a) with a condenser (water vapor is condensed and returned to the reaction system), (b) without a condenser (water vapor is collected and stored in a beaker)

Esterification procedure

Glycerol and acetic acid were heated in certain volumes (according to reactant ratios of 1:3, 1:4, and 1:5 mol of glycerol per mole of acetic acid) in a beaker (for acetic acid) and reactor (for glycerol) until approaching the reaction temperature of 90–120 °C (referring to the study by Sandid et al., 2024). When both reactants reached near the reaction temperature, acetic acid was added to the reactor. The next step was to maintain a stable reaction temperature while running the overhead stirrer at a stirring speed of 700 rpm (referring to studies by Nuryoto et al., 2020; Sandid et al., 2024). When the reactant solution appeared to be completely mixed, a sample was taken for initial acetic acid analysis (A_0) using 0.5 N NaOH solution, which was considered the start of the reaction ($t_0 = 0$ minutes). The next step was to add catalyst into the reactor at 5% of the glycerol mass (Sandid et al., 2024). Next, after 4 hours, the reaction was over, and the sample was retaken to analyze the remaining acetic acid (A_t). To determine the acetic acid conversion, calculations were made using Equation 3, and to determine the percentage of triacetin produced, analysis was performed using GC MS.

$$X_{AA} = \frac{(A_0 - A_t)}{A_0} \times 100\% \quad (3)$$

where: X_{AA} – acetic acid conversion (%), A_0 – acetic acid concentration at $t = 0$ minute (mg/dm^3), A_t – acetic acid concentration at a certain t reaction (mg/dm^3).

To test the mathematical model of reaction kinetics, samples were taken every 1 hour for 4 hours using the same analysis method. All sample analyses were conducted in triplicate and averaged to ensure accurate data.

Characterization techniques

Natural zeolite was characterized using fourier transform infrared spectroscopy (FTIR) type Alpha II from Bruker, Germany, to analyze its functional group peaks and to compare them with existing reference standards. Scanning electron microscope (SEM) using Zeiss – Germany was conducted to observe morphological changes and reinforce the FTIR test results. The surface area analyzer by Quanta Chrome Instruments was used to determine the surface area of zeolite before

and after activation. Additionally, the TPD- NH_3 Autochem II from Micromeritics was employed to assess the acid strength of the zeolite post-activation. Following these analyses, the reaction products were characterized using a GC MS from Thermo Scientific, which includes a Trace ISQ7000 mass spectrometer and a Trace 1310 gas chromatograph. This setup was utilized to analyze the triacetin and its byproducts, monoacetin and diacetin.

Mathematical model testing

To make the observations more comprehensive, this study also conducted a reaction kinetics analysis using a mathematical model. The mathematical model was constructed with several assumptions, including: (a) the catalyst size was assumed to be homogenous, and (b) both external and internal diffusion are very fast, so the reaction rate controls the overall process. Based on these assumptions, the mathematical model was identical to Equation 2, which is the pseudo-homogeneous mathematical model, so Equation 2 could be simplified to Equation 4.

$$\frac{dC_{AA}}{dt} = k C_{AAr}^n \quad (4)$$

where: $\frac{dC_{AA}}{dt}$ – acetic acid reaction rate ($\text{mol}/\text{dm}^3 \text{ h}$), k – reaction rate constant ($1/\text{h}^n$), n – reaction order, C_{AAr} – acetic acid concentration at a certain time (mol/dm^3).

The pseudo-homogeneous model was chosen to predict the reaction rate and reaction rate constant because, in addition to being simple, it often produced good curve fitting between research data and mathematical models. Based on studies conducted by Hazrat et al. (2023) and Morales et al. (2023) this model yielded an R^2 value close to 1, specifically 0.9996, and a residual mean squared error (RMSE) of 1.26×10^{-5} . Therefore, considering the R^2 and RMSE values, this model was potentially quite valid for use in this research case. In this research, reaction orders (n) of 1 and 2 were explored, which are commonly used in general chemical reactions. Equation 4 was modified into first-order and second-order forms as presented in Equation 5 and Equation 6.

$$-\frac{dC_{AA}}{dt} = k C_{AAr} \quad (5)$$

$$-\frac{dC_{AA}}{dt} = k C_{AAr}^2 \quad (6)$$

Equation 5 and Equation 6 can be integrated to obtain Equation 7 and Equation 8.

$$\ln C_{AAr} = \ln C_{AAro} + k t \quad (7)$$

$$\frac{1}{C_{AAr}} = \frac{1}{C_{AAro}} + k t \quad (8)$$

The value will be obtained using Microsoft excel to perform a trendline analysis for the first-order versus the second-order. The mathematical model with an R^2 value close to 1 can be used to describe the phenomenon of the reaction process that occurs and predict conversion under other operating conditions, as well as being applicable for reactor design later.

RESULTS AND DISCUSSION

The effect of pretreatment on changes in natural zeolite characteristics

In Figure 5, the FTIR test results showed that at wave number 1040 cm^{-1} , a very significant peak change occurred (see the circled area in Fig. 5). According to Ferri et al., 2024 and Velarde et al., 2024, wave numbers 1002–1040 represented asymmetric stretching of Si-O and Al-O structures. This peak reduction indicated that the dealumination process had occurred when the zeolite was activated using sulfuric acid (see Fig. 6 referring to the research

of Feng et al., 2019). When surface area analyzer (SAA) testing was conducted using a Quanta chrome Instruments type with the BET method, an increase in surface area of Lampung natural zeolite was observed. The specific surface area initially measured $57.230 \text{ m}^2/\text{gram}$ and increased to $98.738 \text{ m}^2/\text{gram}$ after treatment (Table 2). This increase in specific surface area that occurred in zeolite when pretreated using $6 \text{ N H}_2\text{SO}_4$ indicated that the dealumination process had taken place. The removal of aluminum in the resulted in the formation of spaces, so when the SAA test was performed, and increase in the specific surface area of the Lampung natural zeolite was observed. A similar trend was also seen in the research conducted by Aziz et al. (2019) with the same zeolite (Lampung zeolite), where the Lampung zeolite before pretreatment had a surface area of $48.61 \text{ m}^2/\text{gram}$, and after pretreatment using $1 \text{ M NH}_4\text{Cl}$, the surface area increased to $53.25 \text{ m}^2/$

Table 2. Surface area analysis test results using BET method

Zeolite activity	Surface area (m^2/gram)
Zeolite before pretreatment	57.230
Zeolite after pretreatment using $6 \text{ N H}_2\text{SO}_4$	98.738

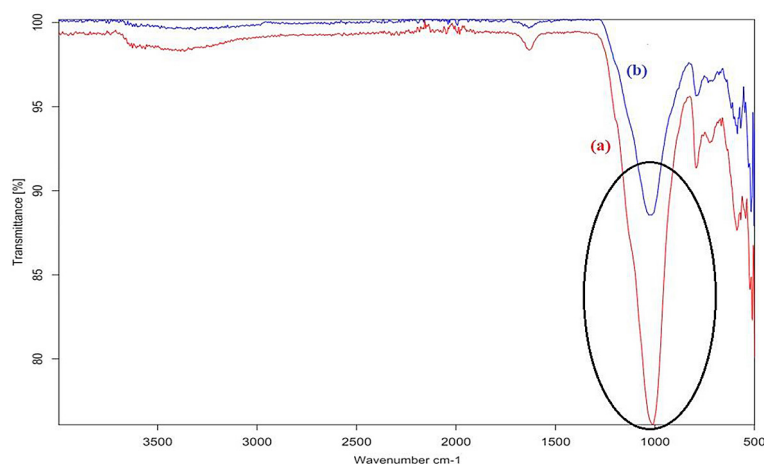


Figure 5. FTIR test results on natural zeolite from Lampung: (a) before pretreatment and (b) after pretreatment

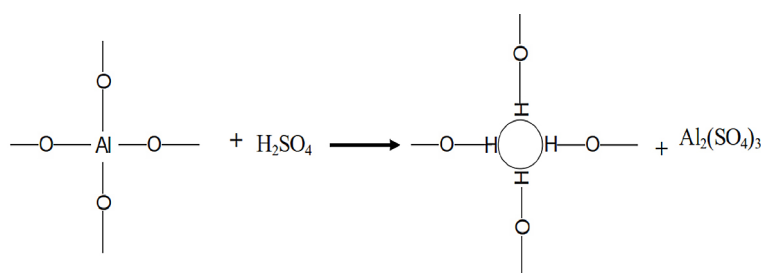


Figure 6. Illustration of the dealumination process of natural zeolite from Lampung, Indonesia

gram. When compared to the research conducted by Sunaryo et al. (2023), the FTIR results in this study showed similarities. The test results of Sunaryo et al. (2023) showed that the Aluminum ion (Al) which was initially 6.16% after pretreatment using NaCl and HCl, decreased to 4.61% and 2.19% respectively. Based on the aluminum test results conducted by Sunaryo et al. (2023), it was concluded that the dealumination process also occurred in this study.

To strengthen the evidence that dealumination had occurred in the zeolite, SEM testing was conducted to examine the morphological surface of the zeolite. The SEM test results showed that the zeolite which had undergone pretreatment had a cleaner and brighter surface compared to the zeolite that had not undergone pretreatment using 6 N H₂SO₄ sulfuric acid (Fig. 7a and Fig. 7b). These SEM results served as evidence that in addition to the dealumination process, such as Na, Mg, and K, had also occurred during the

pretreatment process. The trend of SEM results in this study also had similarities with the SEM results conducted by Sunaryo et al. (2023).

To determine the extent of acidity changes in natural zeolite before and after activation, TPD-NH₃ testing was also conducted. The TPD-NH₃ test results before pretreatment were based on the test results from Aziz et al. (2023) study in the same zeolite. The test results in this study, where zeolite after pretreatment underwent significant changes, showed that untreated Lampung natural zeolite had a peak intensity at temperatures ≤ 200 °C with a TCD signal of 0.085, which decreased to 0.017 after activation (Fig. 8). Meanwhile, at temperatures 400 °C, the TCD signal increased from 0.004 (Aziz et al., 2023) to 0.08 (Fig. 8). According to Khandan and Mashayeki (2023), the higher the intensity of the TCD signal that appeared at temperatures above 400 °C, the greater acidity level.

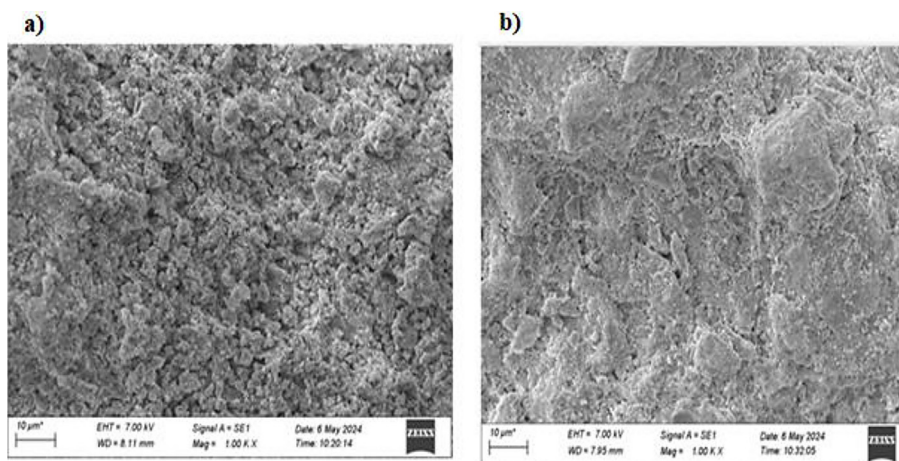


Figure 7. Results of morphological testing using SEM: (a) before pretreatment, (b) after pretreatment using 6 N H₂SO₄

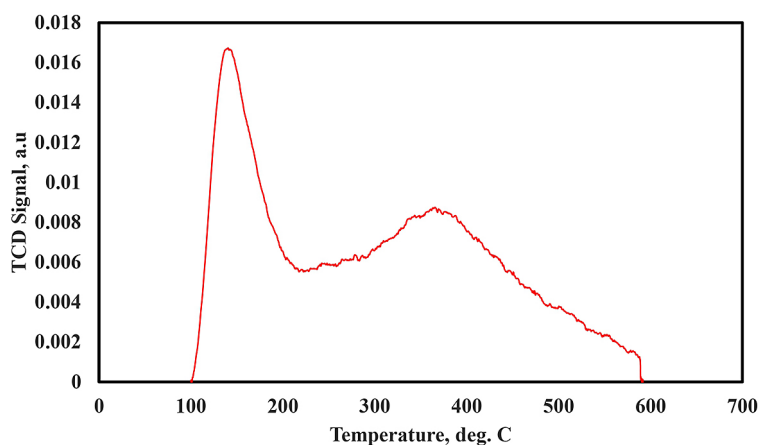


Figure 8. The results of the TPD-NH₃ test on Lampung natural zeolite after pretreatment using 6 N H₂SO₄

Based on the reference from Hasanudin et al. (2024), the acidity test results of natural zeolite from Lampung before pretreatment showed a value of $0.102 \text{ mmol g}^{-1}$. In this study, after pretreatment using $6 \text{ N H}_2\text{SO}_4$, the acidity increased to $2.1706 \text{ mmol g}^{-1}$ (meaning it increased by more than 20 times). Theoretically, the higher the acidity of a catalyst, and this was proven by Hasanudin et al. (2024). The results of the study conducted by Hasanudin et al. (2024) showed that at an acidity of 0.102 mmol/gram , the reactant conversion was 10.23% and the selectivity was 13.23%, while at an acidity of 1.827 mmol/gram , it was able to produce reactant conversion and selectivity of 66.19% and 46.72%, respectively.

Effect of reactant ratio

The increase in the reactant ratio conducted in this study had a positive impact on the conversion of acetic acid produced (Fig. 9). The acetic acid conversion achieved at a reaction time of 4 hours was 26.53, 31.35, and 42.86% (for reactant ratios of 1:3, 1:4, and 1:5 mol of glycerol per mole of acetic acid), respectively. The results of this study are theoretically very logical, because with an increase in the reactant ratio, the interaction between reactions and collisions will increase, and consequently, the reaction rate will also increase (Wanten et al., 2024; Portillo et al., 2023; li et al., 2013). A similar phenomenon to this study was also experienced by Hidayati et al. (2024) who performed an esterification reaction between acetic acid and glycerol, where the conversion increase from 29.94% to 85% based on glycerol for reactant ratios of 1:3 mol of glycerol/ moles of acetic acid and

1:9 mol of glycerol per mole of acetic acid, respectively, conducted at a reaction temperature of 90°C . If observed, the research conducted by Hidayati et al. (2024) resulted in a quite large conversion of 85.5% based on glycerol, but using a ratio of 1:9 mol of glycerol per mole of acetic acid. However, the use of an excessively large reactant ratio becomes a burden on the separation process later and certainly requires a large cost as well.

Different results occurred in Figure 10, with the same reactant ratio as Figure 9. When the chemical reaction temperature was increased to 100°C from the initial condition of 90°C , the acetic acid conversion decreased. According to the Arrhenius equation, increasing the reaction temperature should have increased the reaction rate constant (k) and the reaction rate between acetic acid and glycerol (Equation 2). However, the presence of water as a by-product of the esterification reaction, which was greater in quantity compared to what occurred in Figure 8, caused a significant increase in the reverse reaction. The presence of water in the reaction system caused the reaction to shift to the left (towards the reactants), reducing the amount of ester (triacetin) formed. Additionally, the presence of water also affected the performance of the catalyst itself, as zeolite is a hydrophilic catalyst. Therefore, when the water content in the reaction system was too high, the catalyst activity was disrupted and decreased, inhibiting the reaction process to form triacetin. Observation made by Canhaci et al. (2023) showed that a certain amount of water content in the reaction system impacted the catalyst performance (for hydrophilic catalysts), disrupting the catalyst's function. The resulting impact was a drastic decrease in reactant conversion (Canhaci et al., 2023).

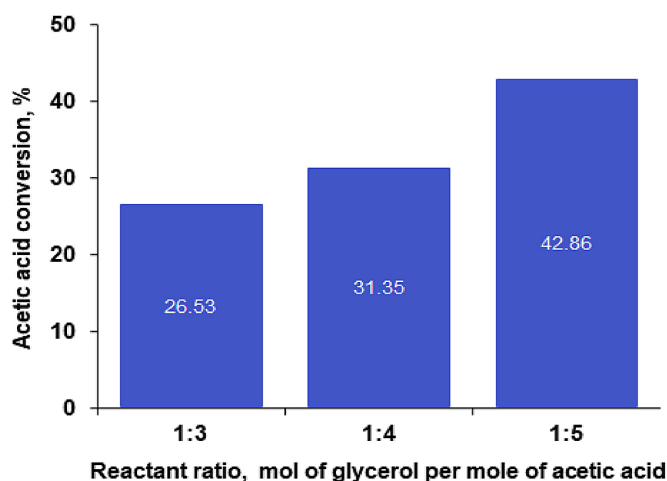


Figure 9. Effect of reactant ratio on acetic acid conversion at reaction temperature of 90°C

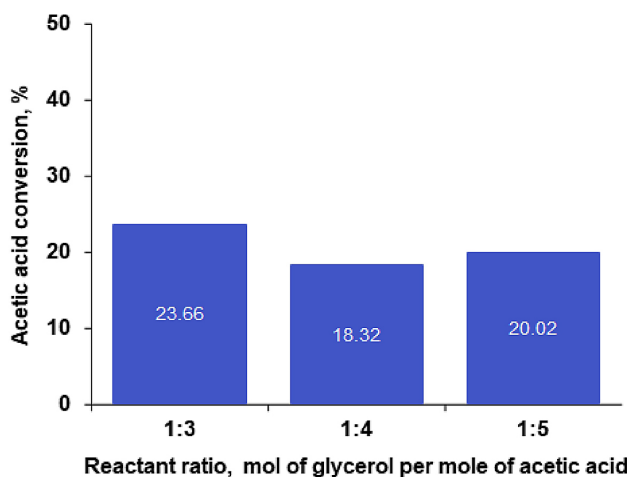


Figure 10. Effect of reactant ratios on acetic acid conversion at reaction temperature of 100 °C

When the water content in the reaction system was sufficiently high, the amount of water adsorbed into the catalyst was also large. Once the adsorption exceeded its maximum limit, catalyst deactivation occurred, and the presence of the catalyst in the reaction system no longer functioned properly. This condition caused the reaction rate and the resulting reactant conversion to decrease significantly. From the data in Figures 9 and Figure 10, it was shown that the presence of water in the reaction system influenced the reaction between acetic acid, glycerol, and the natural zeolite catalyst. Zeolite was hydrophilic (water-loving), while acetic acid and glycerol dissolved well in water, so this condition interfered with the diffusion-reaction process in the triacetin synthesis process. The requirement for a reaction to occur was a good interaction between the reactants (acetic acid-glycerol) and the catalyst (natural zeolite). Therefore, when the reaction system was disturbed, the reaction rate and reactant conversion were also affected.

Effect of reaction temperature

In the observation of the effect of reaction temperature, it was conducted at a fixed reactant ratio of 1:3 mol glycerol/mol acetic acid, as this was the best condition obtained from the observation of reactant ratios (Fig. 9 and Fig. 10). Figure 11 showed that increasing the reaction temperature from 90, 100, and 110 °C had a positive effect on the conversion of acetic acid produced, which was 26.53, 27.66, and 29.94%, respectively, at a reaction time of 4 hours. The results were logically consistent when related to Equation 1 and Equation 2, increasing the reaction temperature increased the diffusion of reactants to the active sites of the catalyst, and when the diffusion process increased, it was automatically followed by an increase in the reaction rate. Research conducted by Foroutan et al., 2023 and Omranpour and Larimi (2024) showed similar phenomena, where when the reaction temperature was raised, the reaction rate increased, resulting in an increase

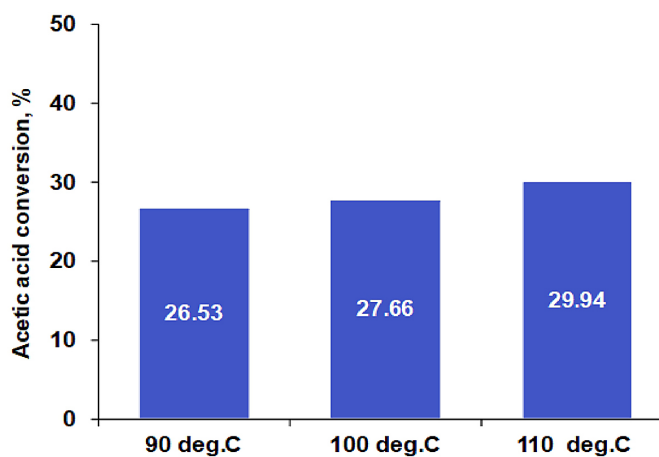


Figure 11. Effect of reaction temperature on the reactant ratio of 1:3 mol of glycerol per mole of acetic acid

in the biodiesel product yield. In general, the rate of esterification reaction between acetic acid and glycerol increased significantly in the first hour (Figs 8–10), then continued to increase but tended to slow down. This occurred due to the presence of water in the reaction system, as previously described and evidenced by Figure 12.

Influence of the reaction with and without water removal from the reaction System

In Figure 12, it was observed that the conversion of acetic acid conducted without a condenser (where water was allowed to evaporate into the environment or water removal was performed from the reaction system) resulted in a significantly higher acetic acid conversion compared to the reaction system with a condenser (where the vapor mixture of water and acetic acid was refluxed back into the reaction system). The sequential acetic acid

conversions produced at a reaction time of 4 hours were 27.66% and 61.87% (an increase of 124%). This result reinforced the phenomena seen in Figure 8 and 9, indicating that the presence of water produced during the reaction process had a significant impact on the reverse reaction and disrupted catalyst performance. Water removal eliminated barriers to reactant diffusion to the catalyst’s active sites and reduced or eliminated water that would have been adsorbed onto the zeolite, allowing the diffusion-reaction process to proceed optimally.

To ensure that the triacetin product was indeed formed, this study conducted testing of the reaction products using GCMS. The GCMS test results performed at a ratio of 1:3 mol of glycerol per mole of acetic acid showed that the triacetin product formed was only 4.94% (Fig. 13 and Table 3). The reaction products were dominated by intermediate products, namely diacetin at 39.96% and a small amount of monoacetin at

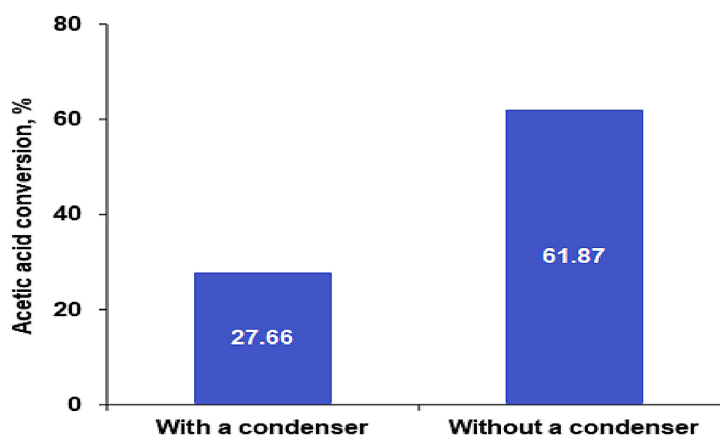


Figure 12. Effect with and without a condenser on the reactant ratio of 1:3 mol of glycerol per mole of acetic acid and reaction temperature of 100 °C

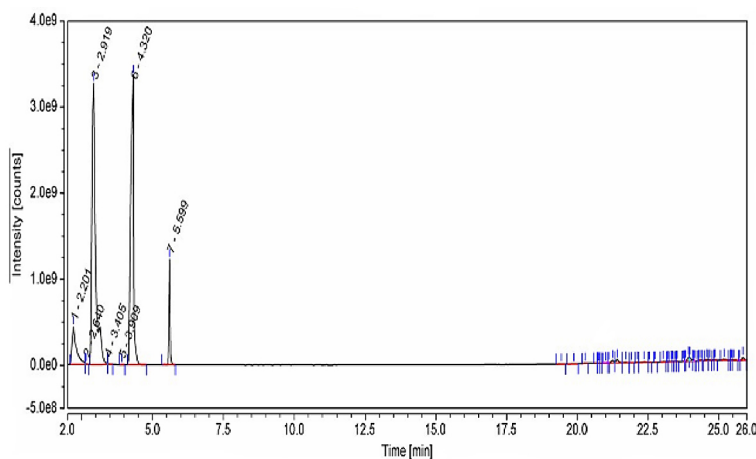


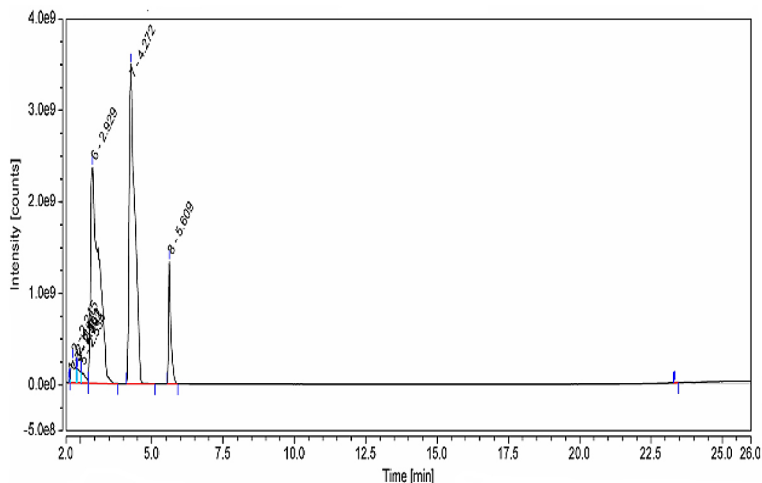
Figure 13. Results of reaction product test using GCMS at 1:3 mol of glycerol per mole of acetic acid without a condenser

Table 3. Relative percentage to area at a ratio of 1:3 mol of glycerol per mole of acetic acid

Peak	Component	Retention time (min)	Area (count x min)	Relative percentage of substance (%)
1 and 2	Acetic acid	2.201 and 2.64	7,7419,720.267 and 61,1317.929	7.51
3	Glycerol	2.92	49,3327,889.895	47.51
4 and 5	Monoacetin	3.405 and 3.91	818,453.120 and 77298.503	0.09
6	Diacetin	4.32	4,148,97718.293	39.96
7	Triacetin	5.60	5,124,9931.272	4.94
Total			1,038,402,329.279	100.00

0.09%. If referring to Figure 1 and Figure 2, stoichiometrically with a reactant ratio of 1:3 mol of glycerol per mole of acetic acid, it should have been sufficient to convert glycerol to triacetin entirely, but this was not the case. Instead, the reaction products seemed to stop at the intermediate product diacetin, and only small amount changed to triacetin. To see the extent of the reactant ratio on the tendency of glycerol to react and the reaction products, an analysis test was also carried out using GCMS for a reactant ratio of 1:4 mol of glycerol per mole of acetic acid. Based on the GCMS test results shown in Figure 14 and Table 4, there was a very significant change, namely the

glycerol which initially at the reactant ratio of 1:4 mol of glycerol per mole of acetic acid (Fig. 14 and Table 4). This data showed that the reaction proceeded faster compared to the reactant ratio of 1:3 mol of glycerol per mole of acetic acid, and much glycerol was consumed to form reaction products. The intermediate product monoacetin formed increased from 0.09% at the reactant ratio of 1:3 mol of glycerol per mole of acetic acid to 43.33% at the reactant ratio of 1:4 mol of glycerol per mole of acetic acid. When referring to the products produced, the products in the form of diacetin and triacetin increased from 39.96% diacetin and 4.94% triacetin for the reactant ratio

**Figure 14.** Test results of reaction products using GCMS at 1:4 mol of glycerol per mole of acetic acid without a condenser**Table 4.** Relative percentage to area at a ratio of 1:4 mol of glycerol per mole of acetic acid

Peak	Component	Retention time (min)	Area (count x min)	Relative percentage substance (%)
1	Acetic acid	2.113	110,2807.463	0.06303
2–5	Glycerol	2.919	82,121,808.910	4.693615
6	Mono acetin	3.405 and 3.909	758,048,988.636	43.32576
7	Diacetin	4.320	79,0631,841.880	45.18801
8	Triacetin	5.599	117,743,998.956	6.729577
Total			1749,649,445,844	100.00

of 1:3 mol of glycerol per mole of acetic acid to 45.19% diacetin and 6.73% triacetin.

The comparison of the two GCMS test results provided information that the step of increasing the reactant ratio from 1:3 mol of glycerol per mole of acetic acid to 1:4 mol of glycerol per mole of acetic acid to increase the triacetin product had a positive impact on the triacetin product produced, although it was not yet optimal, as the increased that occurred was only 1.79%. Therefore, appropriate, effective, and efficient actions were needed to address this problem. If referring to the phenomenon of increasing the reactant ratio, if the step taken was to increase the reactant ratio, then it was possible that the resulting phenomenon would have a similar tendency, where a significant increase in reaction products occurred only in intermediate products such as monoacetin and diacetin, while the increase in triacetin would remain constant. Therefore, a more appropriate method was needed to shift monoacetin and diacetin to triacetin, so that the main product (triacetin) experienced a drastic increase, and the intermediate product in the form of monoacetin became very small. Referring to the case above, the effective method was likely to make 2 series reactors with separation installations installed between them. The product from reactor 1 output was then subjected to removal of water contained in the reaction product output by evaporation to remove the contained water and then reacted again the 2nd reactor by adding acetic acid in certain amount. Under these conditions, the water, which was a by-product and barrier to the reaction, would be eliminated, and the added acetic

acid would fully react with monoacetin and diacetin to form triacetin (Fig. 2).

This step was validated by Pandit et al. (2023) through a simulation using Aspen Plus software that showed when the output of reactor 1 underwent water separation, and was subsequently fed into reactor 2, the triacetin product became maximized. Maximizing the reaction process to obtain a triacetin product approaching 100% is crucial. As seen in Figure 2, monoacetin still has two hydroxyl groups (-OH), and diacetin has one hydroxyl group (-OH). Hydroxyl groups are hygroscopic (water-absorbing), as hydroxyl is highly polar and can form hydrogen bonds with water molecules (Bajuri et al., 2018; Tan et al., 2014). The presence of water in the combustion system can adversely affect the combustion process, resulting in a decrease in the generated heat of combustion, which leads to reduced combustion efficiency and increased combustion delay (Xu et al., 2021), as well as increased deposits during combustion. Additionally, the presence of water will trigger corrosion in the combustion chamber (Olson et al., 2023) and result in increased HC (hydrocarbon) based emissions (Ozsezen et al., 2011). Therefore, maximizing the triacetin product in the reaction process and ensuring that high triacetin purity (above 99%) is added to biodiesel is necessary. This step is taken to minimize the adverse effects of monoacetin and diacetin in the fuel later.

Validation of pseudo-homogeneous model

Figure 15 shows that the longer the reaction time, the lower the acetic acid content in the

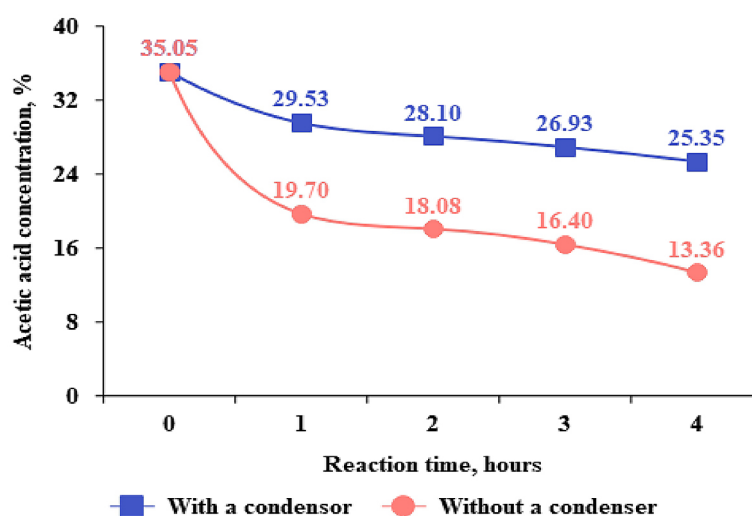


Figure 15. Analysis results over a reaction time range of 1–4 hours at a reaction temperature of 100 °C using reactants with and without a condenser at a reactant ratio of 1:3 mol of glycerol per mole of acetic acid

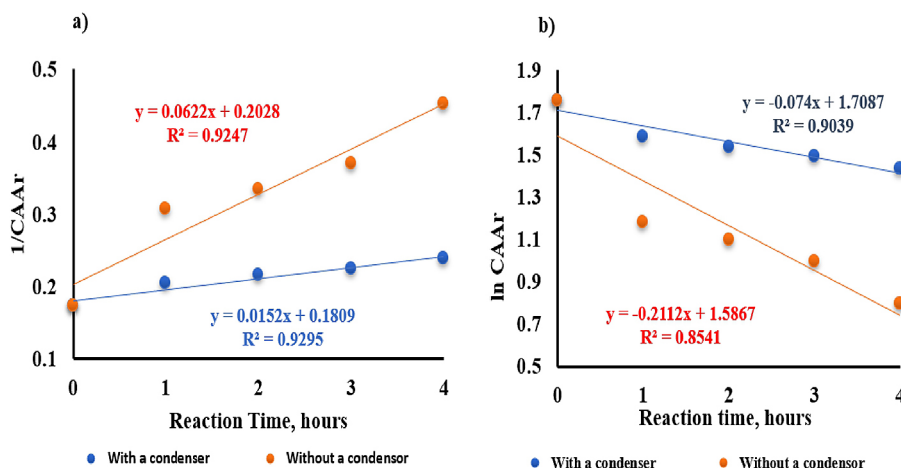


Figure 16. Results of mathematical model calculations using a pseudo-homogeneous approach: (a) first-order, and (b) second-order at a reaction temperature of 100 °C and a reactant ratio of 1:3 mol of glycerol per mole of acetic acid

reaction system. This phenomenon is expected because longer reaction times lead to more reactant molecules interacting and forming products. However, the decrease in acetic acid content in the reaction system without a condenser is much faster compared to the system with a condenser (Fig. 15). In the reaction system with a condenser, at $t = 0$ hours, the acetic acid content was 35.05% and decreased to 29.53, 28.10, 26.93, and 25.53% for reaction times of 1, 2, 3, and 4 hours. Meanwhile, in the reaction without a condenser, the acetic acid content decreased from 35.05% to 19.70, 18.10, 16.40, and 13.36% for 1, 2, 3, and 4 hours respectively. Based on this data, the reaction rate in the system without a condenser (where water is removed from the reaction) is faster than in the system with a condenser (where water is present). The effect of water on the reaction system has been explained in more detail in the previous sub-chapter (see explanations in Fig. 8, Fig. 9, and Fig.10).

The data in Figure 15 was further processed, and calculations were performed based on Equation 7 and Equation 8, resulting in Figure 16. In Figure 16a and Figure 16b, it can be seen that the second-order reaction kinetics model has a higher R^2 value compared to the first-order. For the first-order, the resulting R^2 values are 0.9039 and 0.8541 (for reaction systems with and without condenser, respectively). In contrast, the resulting R^2 values for the second-order are 0.9295 and 0.9247 (for reaction systems with and without condenser, respectively). Based on the R^2 values, this research demonstrates a second-order mathematical model with k values of 0.809612 and

0.928672 $\text{dm}^3 \text{mol}^{-1} \text{h}^{-1}$. Referring to the resulting R^2 values, which are already quite good, this model can be used for operational purposes to quickly predict acetic acid conversion under certain operating conditions, as this model is straightforward. However, the current findings need to be validated with laboratory data. For design purposes, such as reactor design, exploring alternative models like the Langmuir-Hinshelwood or Eley-Rideal models is recommended. These models provide more detailed descriptions of the reaction steps involved (Fig. 2) and can account for consecutive reactions, resulting in R^2 values closer to 1, ideally above 0.99. The goal is to use these constants for reactor design to ensure that the output has minimal deviations and closely reflects actual operating conditions.

CONCLUSIONS

The increase in reactant ratio had both positive (increase in acetic acid conversion) and negative (decrease in acetic acid conversion) impacts, where the positive impact occurred at a reaction temperature of 90 °C and the negative impact at 100 °C. An increase in reaction temperature within the range of 90–110 °C, conducted under stoichiometric conditions of 1:3 mol of glycerol per mole of acetic acid, was followed by an increase in acetic acid conversion. Observations using a reactor without a condenser resulted in a much higher acetic acid conversion compared to one with a condenser (experiencing a 124% increase). This data showed that the water content in the

system affected the resulting acetic acid conversion, and the removal of water from the reaction system had a positive impact on the conversion produced. For future efforts to maximize triacetin production, it was suggested to try using two reactors connected in series, with a water separation process conducted between the two reactors. The pseudo homogeneous model approach could describe the process occurring in triacetin synthesis, with the second-order model being better than the first-order model, as indicated by an average R^2 value above 0.92. However, in the future, other models, such as Langmuir-Hinshelwood or Eley-Rideal, should be explored using a reaction step-based explanation (consecutive reaction) to obtain a reaction kinetics model with an R^2 range of 0.99–1.00. This would allow the resulting constants to be used as design references.

Acknowledgements

The authors express their gratitude to Kemenristekdikti (Ministry of Research, Technology and Higher Education) for the funding provided through the PPS-PTM Grant with contract No: B/761/UN43.9/PT.00.03/2024, enabling this article to be published.

REFERENCES

- Al Muttaqii, M., Marbun, M. P., Priyanto, S., Sibuea, A., Simanjuntak, W., AM, F. S., & Yati, I. (2024). Lampung natural zeolite doped with of ZnO-TiO₂ metal oxide as catalyst for biodiesel production. *Bulletin of Chemical Reaction Engineering & Catalysis*, 19(1), 61–68. <https://doi.org/10.9767/bcrec.20038>
- Amr, A., Salas, A. H., Al-Harbi, N., Basfer, N. M., & Nassr, D. I. (2023). Determination of chemical kinetic parameters in Arrhenius equation of constant heating rate: Theoretical method. *Alexandria Engineering Journal*, 67, 461–472. <https://doi.org/10.1016/j.aej.2022.12.046>
- Awogbemi, O., & Kallon, D. V. V. (2023). Application of machine learning technologies in biodiesel production process – A review. *Frontiers in Energy Research*, 11, 1122638. <https://doi.org/10.3389/fenrg.2023.1122638>
- Aziz, I., Adhani, L., Yolanda, T., & Saridewi, N. (2019). Catalytic cracking of *Jatropha curcas* oil using natural zeolite of Lampung as a catalyst. In *IOP Conference Series: Earth and Environmental Science* 299(1), 012065. IOP Publishing. <https://doi.org/10.1088/1755-1315/299/1/012065>
- Aziz, I., Sugita, P., Darmawan, N., & Dwiatmoko, A. A. (2023). Effect of desilication process on natural zeolite as Ni catalyst support on hydrodeoxygenation of palm fatty acid distillate (PFAD) into green diesel. *South African Journal of Chemical Engineering*, 45(1), 328–338. <https://doi.org/10.1016/j.sajce.2023.07.002>
- Azmi, N., Ameen, M., Yashni, G., Yusup, S., Mohd Yusoff, M. H., & Chai, Y. H. (2023). In situ catalytic conversion of glycerol to triacetin under microwave irradiation with commercial palladium on activated carbon catalyst. *Journal of Sustainable Development of Energy, Water and Environment Systems*, 11(4), 1–17. <https://doi.org/10.13044/j.sdwes.d11.0465>
- Bajuri, F., Mazlan, N., & Ishak, M. R. (2018). Water absorption analysis on impregnated kenaf with nanosilica for epoxy/kenaf composite. In *IOP Conference Series: Materials Science and Engineering* 405(1), 012013. IOP Publishing. <https://doi.org/10.1088/1757-899X/405/1/012013>
- Britto, P. J., Kulkarni, R. M., Narula, A., Poonacha, S., Honnatagi, R., Shivanathan, S., & Wahab, W. (2022). Optimization and packed bed column studies on esterification of glycerol to synthesize fuel additives-acetins. *Korean Chemical Engineering Research*, 60(1), 70–79.
- Çakmak, A (2021). Investigation of using triacetin as biofuel in a diesel engine through combustion, performance, emissions, and cost analysis. *International Symposium on Automotive Science and Technology*, Ankara Turkey.
- Canhaci, S. J., Albuquerque, E. M., Lopes, C. C., Faria, V. W., Chinelatto Junior, L. S., Duarte de Farias, A. M., & Fraga, M. A. (2023). Balance between catalyst acidity and hydrophilicity in biofuel production from fatty acid esterification over Al-SBA-15. *Catalysis*, 13(5), 827. <https://doi.org/10.3390/catal13050827>
- Elsayed, M., Eraky, M., Osman, A. I., Wang, J., Farghali, M., Rashwan, A. K., & Abomohra, A. (2024). Sustainable valorization of waste glycerol into bioethanol and biodiesel through biocircular approaches: a review. *Environmental Chemistry Letters*, 22(2), 609–634. <https://doi.org/10.1007/s10311-023-01671-6>
- Eremeeva, A. M., Kondrasheva, N. K., Khasanov, A. F., & Oleynik, I. L. (2023). Environmentally friendly diesel fuel obtained from vegetable raw materials and hydrocarbon crude. *Energies*, 16(5), 2121. <https://doi.org/10.3390/en16052121>
- Feng, A., Yu, Y., Mi, L., Cao, Y., Yu, Y. & Song, L. (2019). Synthesis and characterization of hierarchical Y zeolites using NH₄HF₂ as dealumination agent. *Microporous and Mesoporous*

- Materials*, 280, 211–218. <https://doi.org/10.1016/j.micromeso.2019.01.039>
14. Ferri, B. B., Wernke, G., Resende, J. F., Ribeiro, A. C., Cusioli, L. F., Bergamasco, R., & Vieira, M. F. (2024). Natural zeolite as adsorbent for metformin removal from aqueous solutions: Adsorption and regeneration properties. *Desalination and Water Treatment*, 320, 100602. <https://doi.org/10.1016/j.dwt.2024.100602>
 15. Foroutan, R., Peighambaroust, S. J., Mohammadi, R., Peighambaroust, S. H., & Ramavandi, B. (2023). Investigation of kinetics, thermodynamics, and environmental factors of biodiesel generation from sunflower and castor oil using rice husk ash/CuO/K₂CO₃ heterogeneous catalyst. *Environmental Technology & Innovation*, 32, 103307. <https://doi.org/10.1016/j.eti.2023.103307>
 16. Fogler H.S (2006). Elements Of Chemical Reaction Engineering. 4th Edition, Prentice Hall, Upper Saddle River.
 17. Hasanudin, H., Asri, W. R., Rahmawati, R., Riyanti, F., Maryana, R., Al Muttaqii, M.,... & Novia, N. (2024). Conversion of Isopropanol to Diisopropyl Ether over Cobalt Phosphate Modified Natural Zeolite Catalyst. *Bulletin of Chemical Reaction Engineering & Catalysis*, 19(2), 275–284. <https://doi.org/10.9767/brec.20144>
 18. Hazrat, M. A., Rasul, M. G., Khan, M. M. K., Ashwath, N., Fattah, I. M. R., Ong, H. C., & Mahlia, T. M. I. (2023). Biodiesel production from transesterification of Australian Brassica napus L. oil: Optimisation and reaction kinetic model development. *Environment, Development and Sustainability*, 25(11), 12247–12272. <https://doi.org/10.1007/s10668-022-02506-0>
 19. Hidayati, N., Khoiruddin, W., Purnama, H., & Edfendy, M. (2024). Synthesis and Characterisation of Graphene Oxide Catalysts for Glycerol Acetylation. *Bulletin of Chemical Reaction Engineering & Catalysis*, 19(2), 340–349. <https://doi.org/10.9767/brec.20146>
 20. Intang, A., Susmanto, P., Bustan, M. D., & Haryati, S. (2024). Determination of swelling operation parameters to improve the hierarchy of natural zeolite lampung after synthesis. *South African Journal of Chemical Engineering*. <https://doi.org/10.1016/j.sajce.2024.08.004>
 21. Jagadish, T., Ramudu, M. P., Swapna, S., Challa, P., Rao, M. V., Vinod, G., & Manjari, P. S. (2025). Synthesis of sustainable biochar acid catalyst by utilization of palmyra palm fruit shell waste biomass and application to glycerol esterification. *Journal of Molecular Liquids*, 127039. <https://doi.org/10.1016/j.molliq.2025.127039>
 22. Kalyani, T., Prasad, L. S. V., & Kolakoti, A. (2023). Effect of triacetin as an oxygenated additive in algae biodiesel fuelled CI engine combustion, performance, and exhaust emission analysis. *Fuel*, 338, 127366. <https://doi.org/10.1016/j.fuel.2022.127366>
 23. Khalaf, M., Xuan, T., Abdel-Fadeel, W. A., Mustafa, H. M., Abdelhady, S., & Esmail, M. F. (2024). A comparative study of diesel engine fueled by Jatropha and Castor biodiesel: Performance, emissions, and sustainability assessment. *Process Safety and Environmental Protection*, 188, 453–466. <https://doi.org/10.1016/j.psep.2024.05.137>
 24. Khandan, N., & Mashayekhi, M. (2023). Investigation of the effect of Cu-based catalyst acidity on Hydrogen production from the water-gas shift reaction. *Iranian Journal of Chemistry and Chemical Engineering*, (Articles in Press).
 25. Kulkarni, R. M., Britto, P. J., Narula, A., Saqline, S., Anand, D., Bhagyalakshmi, C., & Herle, R. N. (2020). Kinetic studies on the synthesis of fuel additives from glycerol using CeO₂-ZrO₂ metal oxide catalyst. *Biofuel Research Journal*, 7(1), 1100–1108. <https://doi.org/10.18331/BRJ2020.7.1.2>
 26. Li, D., Rohani, V., Ramaswamy, A. P., Sennour, M., Georgi, F., Dupont, P., & Fulcheri, L. (2023). Orientating the plasma-catalytic conversion of CO₂ and CH₄ toward liquid products by using a composite catalytic bed. *Applied Catalysis A: General*, 650, 119015. <https://doi.org/10.1016/j.apcata.2022.119015>
 27. Morales, P. C., García-Martín, A., & Ladero, M. (2023). Pectooligosaccharides rich in galacturonic acid produced from Orange Processing Waste by autohydrolysis: Process optimization and kinetic analysis. *Bioresource Technology Reports*, 21, 101369. <https://doi.org/10.1016/j.biteb.2023.101369>
 28. Nindya, C. C. S., Anggara, D. R., & Teguh, K. (2020). Esterification glycerol (by product in biodiesel production) with oleic acid using mordenite natural zeolite as catalyst: study of reaction temperature and catalyst loading effect. In *IOP Conference Series: Materials Science and Engineering* 909(1), 012001. IOP Publishing.
 29. <https://doi.org/10.1088/1757-899X/909/1/012001>
 30. Nuryoto, N., Amaliah, A. R., Puspitasari, A., & Ramadhan, A. D. (2020). Study of Esterification Reaction Between Ethanol and Acetic Acid Using Homogeneous and Heterogeneous Catalyst. *World Chemical Engineering Journal*, 4(2), 51–55. <https://doi.org/10.48181/wcej.v4i2.8952>
 31. Okonye, L. U., Yao, Y., Ren, J., Liu, X., & Hildebrandt, D. (2023). A perspective on the activation energy dependence of the Fischer-Tropsch synthesis reaction mechanism. *Chemical engineering science*, 265, 118259. <https://doi.org/10.1016/j.ces.2022.118259>
 32. Olson, A. L., Tunér, M., & Verhelst, S. (2023). A review of isobutanol as a fuel for internal combustion

- engines. *Energies*, 16(22), 7470. <https://doi.org/10.3390/en16227470>
33. Omranpour, S., & Larimi, A. (2024). Modeling and simulation of biodiesel synthesis in fixed bed and packed bed membrane reactors using heterogeneous catalyst: a comparative study. *Scientific Reports*, 14(1), 10153. <https://doi.org/10.1038/s41598-024-60757-5>
34. Ozsezen, A.N.; Turkcan, A.; Sayin, C.; Canakci, M. (2011). Comparison of performance and combustion parameters in a heavy-duty diesel engine fueled with iso-butanol/diesel fuel blends. *Energy Explor. Exploit.*, 29, 525–541. <https://doi.org/10.1260/0144-5987.29.5.525>
35. Pandit, K., Jeffrey, C., Keogh, J., Tiwari, M. S., Artioli, N., & Manyar, H. G. (2023). Techno-economic assessment and sensitivity analysis of glycerol valorization to biofuel additives via esterification. *Industrial & Engineering Chemistry Research*, 62(23), 9201–9210. <https://doi.org/10.1021/acs.iecr.3c00964>
36. Portillo, A., Parra, O., Ereña, J., Aguayo, A. T., Bilbao, J., & Ateka, A. (2023). Effect of water and methanol concentration in the feed on the deactivation of In₂O₃-ZrO₂/SAPO-34 catalyst in the conversion of CO₂/CO to olefins by hydrogenation. *Fuel*, 346, 128298. <https://doi.org/10.1016/j.fuel.2023.128298>
37. Putera, A. D. P., Avarmaa, K., Petrus, H. T. B. M., Brooks, G. A., & Rhamdhani, M. A. (2024). On the diffusivity of boron in slag during silicon refining. *Journal of Sustainable Metallurgy*, 1–9. <https://doi.org/10.1007/s40831-024-00882-7>
38. Rahmat, N., Abdullah, A. Z., & Mohamed, A. R. (2010). Recent progress on innovative and potential technologies for glycerol transformation into fuel additives: A critical review. *Renewable and Sustainable Energy Reviews*, 14(3), 987-1000. <https://doi.org/10.1016/j.rser.2009.11.010>
39. Ramadhan, A. D., Carolina, N., Nuryoto, N., & Kurniawan, T. (2019). The use of natural zeolite as a catalyst for esterification reaction between glycerol and oleic acid. *Reaktor*, 19(4), 172–179. <https://doi.org/10.14710/reaktor.19.4.172-179>
40. Sandid, A., Attarbach, T., Navarro-Tovar, R., Pérez-Page, M., Spallina, V., & Esteban, J. (2024). Production of triacetin from industrially derived purified glycerol: Experimental proof of concept, kinetic model derivation and validation. *Chemical Engineering Journal*, 496, 153905. <https://doi.org/10.1016/j.cej.2024.153905>
41. Sriratchawan, P., Eaimsumang, S., & Luengnaruemitchai, A. (2022). Triacetin Production from Acetylation of Glycerol: A Review. *Proceedings of the 2022 Sustainable Research and Innovation Conference - JKUAT Main Campus, Kenya*.
42. Sunaryo, S., Suyitno, S., Arifin, Z., Setiyo, M., & Diharja, F. P. (2023). Thermal Stability and Surface Area Modification of Natural Zeolite Through HCl & NaCl Treatment to Apply in Pyrolysis Systems. In *E3S Web of Conferences 465*, 01026. EDP Sciences. <https://doi.org/10.1051/e3sconf/202346501026>
43. Tan, B. K., Ching, Y. C., Gan, S. N., Ramesh, S., & Rahman, M. R. (2014). Water absorption properties of kenaf fibre–poly (vinyl alcohol) composites. *Materials Research Innovations*, 18(sup6), S6-144. <https://doi.org/10.1179/1432891714Z.000000000946>
44. Tasuna, N., & Hidayatillah, K. H. (2021). Selective esterification of glycerol diacetin and triacetin over rice husk biosilica catalyst with microwave heating. In *IOP Conference Series: Materials Science and Engineering 1087*(1), 012063. IOP Publishing. <https://doi.org/10.1088/1757-899X/1087/1/012063>
45. Velarde, L., Escalera, E., & Akhtar, F. (2024). Surfactant-modified Bolivian natural zeolite for the adsorption of Cr (VI) from water. *Water*, 16(14), 1954. <https://doi.org/10.3390/w16141954>
46. Wanten, B., Gorbanev, Y., & Bogaerts, A. (2024). Plasma-based conversion of CO₂ and CH₄ into syngas: A dive into the effect of adding water. *Fuel*, 374, 132355. <https://doi.org/10.1016/j.fuel.2024.132355>
47. Wirawan, S. S., Solikhah, M. D., Setiaprada, H., & Sugiyono, A. (2024). Biodiesel implementation in Indonesia: Experiences and future perspectives. *Renewable and Sustainable Energy Reviews*, 189, 113911. <https://doi.org/10.1016/j.rser.2023.113911>
48. Yanti, N. R., Heryani, H., Putra, M. D., & Nugroho, A. (2019). Triacetin production from glycerol using heterogeneous catalysts prepared from peat clay. *International Journal of Technology*, 10(5), 970–978. <https://doi.org/10.14716/ijtech.v10i5.2685>
49. Yadav, G. D., & Katole, S. O. (2025). Synthesis of green bioadditives via esterification of glycerol with acetic acid catalysed by modified heteropolyacid on clay support. *Journal of the Indian Chemical Society*, 101623. <https://doi.org/10.1016/j.jics.2025.101623>